RSC Advances

PAPER

View Article Online
View Journal | View Issue

Cite this: *RSC Adv.*, 2015, **5**, 107793

Synthesis and properties of hyperbranched polyimides derived from tetra-amine and long-chain aromatic dianhydrides†

Shanyou Liu,[a] Yunhe Zhang,[a] Xueping Wang,[b] Haiwei Tan,[a] Ningnig Song[a] and Shaowei Guan*[a]

To investigate the properties of hyperbranched polyimides (HBPIs) for potential optical applications, novel fluorinated tetra-amine monomers with ether and sulfonyl groups, 4,4′-di[3,5-di(2-trifluoromethyl-4-aminophenoxy)phenoxy]sulfone, and five kinds of long-chain dianhydrides, have been designed and synthesized. A series of anhydride-terminated hyperbranched polyimides have been prepared *via* a two-step method with chemical imidization. The HBPIs possess outstanding solubility and show excellent thermal and optical properties. The glass transition temperatures (T_g) of the HBPIs range from 230–242 °C determined by differential scanning calorimetry (DSC), and 232–263 °C by thermomechanical analysis (TMA), depending on the dianhydride used. The 5% weight loss temperatures are in the range of 480–533 °C, showing high intrinsic thermal-resistant characteristics of the HBPIs. The HBPI films show good optical transparency, higher than 80% at 800 nm. The cast polyimide films have favorable mechanical properties with tensile strengths of 91–112 MPa, elongation at break of 5.99–7.99%, and initial modulus of 2.14–2.57 GPa. The polyimides exhibit average refractive indices of 1.5780–1.6271, and birefringence of 0.0065–0.0079 because of the hyperbranched structure. The PI derived from 2,2-bis[4-(3,4-dicarboxyphenoxy)phenyl]hexafluoropropane possesses the lowest refractive indices due to the high fluorine content in the polymer chain.

Received 4th November 2015
Accepted 11th December 2015

DOI: 10.1039/c5ra23227a

www.rsc.org/advances

1. Introduction

Aromatic polyimides (PIs) that are known for their excellent physical and chemical properties have been researched and developed for many years for both their academic and technical interest.[1–5] Polyimide materials are particularly attractive in integrated optical components and circuits for high speed optical communication, due to their high performance, rapid processability and cost-effectiveness compared to silica.[6,7] Especially, fluorinated polyimides have been introduced as candidates for direct on-chip interconnection and optical devices, because they have low optical loss at the communication wavelengths, a broad range of refractive indices and excellent heat resistance.[8–11] Although a variety of PIs for optical applications have been reported, the unneglectable birefringence caused by the rigid molecular chains restricts their applications.[11,12]

Hyperbranched polyimides are a relatively new class of macromolecules which have attracted much attention for their unique treelike randomly branching architecture and amounts of terminal groups since Flory's seminal theoretical report in 1952.[13,14] Hyperbranched polyimides do not own the well-defined architectures as dendrimers since the dendrimers synthesis involves multistep procedures (protection, coupling, and deprotection cycles), which leads to high cost and problems in large-scale preparation. The hyperbranched polyimides can be simply prepared by direct "one-step" polymerization of multi-functional monomers. Nevertheless, hyperbranched polyimides are thought to have similar physical properties to dendrimers and can be used to replace dendrimers for most cases.[15–17] The isotropic globular structure endows the polymer low birefringence values. In addition, the HBPIs possess controllable and invariable refractive index as the employment of different dianhydrides, which is fundamental and important for materials in optical applications.[12]

Hyperbranched polyimides (HBPIs) have been prepared from either AB_n ($n \geq 2$) monomers or $A_2 + B_m$ ($m \geq 3$) monomers, where A represents anhydride functional group and B represents amino functional group.[18–20] It is known that hyperbranched polymers have poor mechanical properties probably due to a considerably lower number of physical entanglements between the macromolecules.[21,22] As a result, the distances among

[a]*Alan G. MacDiarmid Laboratory, College of Chemistry, Jilin University, Qianjin Road 2699, Changchun 130012, People's Republic of China. E-mail: guansw@jlu.edu.cn*
[b]*Optoelectronic Information Science and Technology Department, College of Science, Changchun University of Science and Technology, Weixing Road 7089, Changchun 130022, People's Republic of China*

† Electronic supplementary information (ESI) available. See DOI: 10.1039/c5ra23227a

branches and flexibility in relative rigid branched structure affect the intermolecular entanglements significantly. In this work, a novel tetra-amine 4,4′-di[3,5-di(2-trifluoromethyl-4-aminophenoxy)phenoxy]sulfone has been successfully synthesized, as well as five kinds of long-chain dianhydrides, which was intended to increase the chain entanglements thus improve the mechanical properties of HBPIs, in addition, the different linkage bonds of dianhydrides endow the tunable refractive indice. Subsequently, a series of anhydride-terminated polyimides have been prepared. All the polyimides exhibited excellent solubility, high glass transition temperatures, favorable mechanical properties, and low birefringences.

2. Experimental

2.1. Materials

Boron tribromine (BBr_3), hydroquinone, 4,4′-thiodiphenol, 4,4′-dihydroxybiphenyl, 4,4′-dihydroxydiphenyl ether, 4-nitrophthalonitrile, and 4,4′-(hexafluoroisopropylidene)diphenol were purchased from Aladdin Corporation, and used as received. 2-Chloro-5-nitrobenzotrifluoride, 4,4′-dichlorophenyl sulfone and 3,5-dimethoxyphenol were purchased from Tokyo Chemical Industry Co. Ltd. *N*,*N*-Dimethylacetamide (DMAc) was distilled under reduced pressure over calcium hydride and stored over 4 Å molecular sieves. Other solvents and reagents were obtained from Sinopharm Chemical Reagent Co. Ltd and used as received.

2.2. Characterization

The FT-IR spectra (KBr) were measured by a Nicolet Impact 410 Fourier transform infrared spectrometer. ^{1}H NMR spectra were determined on a Bruker AVANCE NMR spectrometer (300 MHz) with tetramethylsilane as a reference. Gel permeation chromatograms (GPC) employing polystyrene as a standard were obtained through an Agilent PL-GPC220 with *N*,*N*-dimethylformamide (DMF) as an eluent at a flow rate of 1 mL min^{-1}. Intrinsic viscosity was measured on an Ubbelohde viscometer in thermostatic container in *N*,*N*-dimethylacetamide (DMAc) at 25 °C. Differential scanning calorimetry (DSC) measurements were conduct on a Mettler Toledo DSC 821^e instrument at a heating rate of 10 °C min^{-1} under nitrogen. Thermal gravimetric analyses (TGA) were carried out under nitrogen atmosphere at a heating rate of 10 °C min^{-1} and polymers were contained within open platinum pans on a PERKIN ELMER TGA-7. The mechanical tests in tension were performed using a SHIMADZU AG-I at a constant crosshead speed of 10 mm min^{-1}. Water absorption of the films was measured by a Mettler microbalance with a sensitivity of 10^{-5} g after immersing the membranes into double-distilled water for 72 h at room temperature. In-plane (n_{TE}) and out-of-plane (n_{TM}) refractive indices of the polyimides were measured with a Metricon Model 2010 prism coupler equipped with a half-wave plate in the light path and a He–Ne laser light source (wavelength: 632.8 nm). The birefringences (Δn) were calculated as a difference between n_{TE} and n_{TM}. The average refractive index was calculated according to the equation $n_{av} = [(2n_{TE}^2 + n_{TM}^2)/3]^{1/2}$. The coefficient of thermal expansion (CTE) of the PI films was determined by a thermal mechanical analysis (TMA) using a thermomechanical analyzer TMA/SDTA841e (Mettler Toledo) at a heating rate of 10 °C min^{-1}. The CTE values were calculated as a mean coefficient of linear thermal expansion in the temperature range of 25–220 °C. UV transmittance were measured by a Shimadzu UV 2501 PC spectrophotometer. The PANalytical B.V. Empyrean X-ray Diffractometer (Cu Kα radiation) was used for measuring morphology of HBPI films. The dielectric constants were obtained from Hewlett-Packard 4285A at the room temperature with the conductive silver coating on the surface of polyimide films.

2.3. Monomer synthesis

4,4′-Di(3,5-dimethoxyphenoxy)sulfone (I). A mixture of 4,4′-dichlorophenyl sulfone (10.05 g, 0.035 mol), 3,5-dimethoxyphenol (10.78 g, 0.07 mol), anhydrous K_2CO_3 (5.80 g, 0.042 mol), *N*,*N*-dimethylacetamide (100 mL), and toluene (40 mL) was added into a three-necked, 250 mL, round-bottom flask fitted with a mechanical stirrer, a nitrogen inlet pipet, and a Dean–Stark trap and a condenser. Then the mixture was heated to 140 °C in nitrogen for 4 h with stirring to facilitate dehydration. When the water was completely removed, the residual toluene was distilled off. Subsequently, the mixture was heated to 150 °C and maintained at this temperature for 16 h. After cooling to room temperature, the mixture was poured into deionized water (1 L) to give yellow precipitate. The precipitate was collected by filtration, washed with water, and dried in vacuum. The product was recrystallized from ethanol to give yellow block crystals. Yield: 16.44 g (90%). Mp: 122 °C (DSC peak temperature). FT-IR (KBr, cm^{-1}): 2977, 2838 (–CH_3), 1319, 1153 (O═S═O), 1279, 1237 (Ph–O–Ph). ^{1}H NMR (300 MHz, DMSO-d_6, ppm): 7.932–7.903 (d, J = 8.7 Hz, 4H), 7.142–7.112 (d, J = 9 Hz, 4H), 6.420–6.405 (t, 2.4 Hz, 2H), 6.308–6.300 (d, J = 2.4 Hz, 4H), 3.724 (s, 12H).

4,4′-Di(3,5-dihydroxyphenoxy) sulfone (II). A mixture of 4,4′-di(3,5-dimethoxyphenoxy)sulfone (15.66 g, 0.03 mol) and dichloromethane (40 mL) was added to a three-necked, 1000 mL, round-bottom flask equipped with a mechanical stirrer, a nitrogen inlet and a dropping funnel. The solution was controlled at −10 °C, and the BBr_3 solution of dichloromethane (1 mol L^{-1}, 300 mL) was dropped slowly through the dropping funnel in 3 h. The mixture was held at this temperature for 6 h. Subsequently, the mixture was quenched through water (20 mL) adding, and then poured into saturated $NaHCO_3$ aqueous solution (1000 mL) to neutralize the by-product HBr. The precipitate was collected by filtration, washed with water, and dried in vacuum. The product was recrystallized from ethanol and water to give deep yellow crystals. Yield: 12.44 g (89%). Mp: 162 °C (DSC peak temperature). FT-IR (KBr, cm^{-1}): 3433–3249 (O–H), 1311, 1153 (O═S═O), 1288, 1233 (Ph–O–Ph). ^{1}H NMR (300 MHz, DMSO-d_6, ppm): 9.565 (s, 4H, OH), 7.929–7.900 (d, J = 8.7 Hz, 4H), 7.142–7.112 (d, J = 9 Hz, 4H), 6.095–6.082 (t, 2.1 Hz, 2H), 5.908–5.901 (d, J = 2.1 Hz, 4H).

4,4′-Di[3,5-di(2-trifluoromethyl-4-nitrophenoxy)phenoxy] sulfone (III). A mixture of 4,4′-di(3,5-dihydroxyphenoxy)sulfone (6.99 g, 0.015 mol), anhydrous K_2CO_3 (4.97 g, 0.036 mol), *N*,*N*-dimethylacetamide (100 mL), and toluene (40 mL) was added to a three necked, 250 mL, round-bottom, flask fitted with

a mechanical stirrer, a nitrogen inlet, a Dean–Stark trap, and a condenser. The mixture was heated to 140 °C for 6 h in nitrogen to facilitate dehydration. When the water was completely removed, the mixture was heated to 150 °C and maintained for 6 h to distill off the residual toluene. Subsequently 2-chloro-5-nitrobenzotrifluoride (13.53 g, 0.06 mol) was added into the flask when the mixture was cooled to room temperature. The mixture was maintained at 120 °C for 16 h. Again the mixture was cooled to room temperature and poured into deionized water (1 L) to give yellow precipitate, which was collected and washed thoroughly with deionized water to give a crude product. Then the solid was purified by recrystallization from acetonitrile. Yield: 13.01 g (71%). Mp: 145 °C (DCS peak temperature). FT-IR (KBr, cm^{-1}): 1533, 1354 (–NO_2), 1333, 1157 (O═S═O), 1290, 1244 (Ph–O–Ph), 1147, 1117 (C–F). ^{1}H NMR (300 MHz, DMSO-d_6, ppm): 8.515–8.484 (m, 8H), 7.983–7.954 (d, J = 8.7 Hz, 4H), 7.464–7.431 (d, J = 9.9 Hz, 4H), 7.303–7.273 (d, J = 9 Hz, 4H), 7.140–7.126 (t, 2.1 Hz, 2H), 7.082–7.075 (d, J = 2.1 Hz, 4H).

4,4′-Di[3,5-di(2-trifluoromethyl-4-aminophenoxy)phenoxy] sulfone (IV). A mixture of 4,4′-di[3,5-di(2-trifluoromethyl-4-nitrophenoxy)phenoxy]sulfone (12.22 g, 0.01 mol), 10% Pd/C (0.20 g), ethanol (100 mL) was added to a three-necked, 250 mL, round-bottom flask equipped with a mechanical stirrer, a nitrogen inlet and a condenser. When the mixture was heated at boiling temperature, the hydrazine monohydrate (15 mL) was added dropwise in 2 hours. Then the mixture was maintained at the boiling temperature for 8 h. The resulted clear, darkened solution was filtered at room temperature to remove Pd/C, and the filtrate was then distilled to remove most of the solvent, subsequently poured into deionized water to give light yellow precipitate which was washed thoroughly to remove unreacted hydrazine monohydrate. Yield: 10.03 g (91%). mp: 97 °C (DSC peak temperature). FT-IR (KBr, cm^{-1}): 3469, 3386 (–NH_2), 1340, 1166 (O═S═O), 1263, 1221 (Ph–O–Ph), 1149, 1117 (C–F). ^{1}H NMR (300 MHz, DMSO-d_6, ppm): 7.924–7.895 (d, J = 8.7 Hz, 4H), 7.152–7.122 (d, J = 9 Hz, 4H), 6.965–6.936 (d, J = 8.7, 4H), 6.873–6.864 (d, J = 2.7 Hz, 8H), 6.809–6.771 (dd, J = 8.7 Hz, 2.7 Hz, 4H), 6.254–6.247 (d, J = 2.1 Hz, 4H), 6.176–6.161 (t, 2.1 Hz, 2H), 5.511 (s, 8H).

1,4-Bis(3,4-dicarboxyphenoxy)benzene (1). (1) was synthesized according to the literature.[23] Yield: 76%. Mp: 268 °C (DSC peak temperature). FT-IR (KBr, cm^{-1}): 1844, 1774 (C═O), 1275, 1217 (C–O–C). ^{1}H NMR (300 MHz, DMSO-d_6, ppm): 8.121–8.094 (d, J = 8.1, 2H), 7.633–7.625 (d, J = 2.4, 2H), 7.605–7.584 (dd, J = 2.1 Hz, 4.5 Hz, 2H), 7.358 (s, 4H).

4,4′-[Sulfonyl-bis(1,4-phenylene)dioxy]diphthalic anhydride (2). (2) was synthesized according to the literature.[23] Yield: 72%. Mp: 253 °C (DSC peak temperature). FT-IR (KBr, cm^{-1}): 1845, 1776 (C═O), 1325, 1148 (O═S═O), 1281, 1230 (C–O–C). ^{1}H NMR (300 MHz, DMSO-d_6, ppm): 8.146–8.118 (d, J = 8.4 Hz, 2H), 8.098–8.068 (d, J = 9 Hz, 4H), 7.776–7.769 (d, J = 2.1 Hz, 2H), 7.689–7.654 (dd, J = 2.1 Hz, 8.4 Hz, 2H), 7.366–7.337 (d, J = 8.7 Hz, 4H).

2,2-Bis[4-(3,4-dicarboxyphenoxy)phenyl]hexafluoropropane (3). (3) was synthesized according to the literature.[23] Yield: 81%. Mp: 233 °C (DSC peak temperature). FT-IR (KBr, cm^{-1}): 1850, 1780 (C═O), 1282, 1228 (C–O–C), 1181, 1142 (C–F). ^{1}H NMR (300 MHz, DMSO-d_6, ppm): 8.140–8.112 (d, J = 8.4 Hz, 2H), 7.663–7.641 (q, J = 2.1 Hz, 4H), 7.621–7.614 (d, J = 2.1 Hz, 2H), 7.535–7.506 (d, J = 8.7 Hz, 4H), 7.337–7.308 (d, J = 8.7 Hz, 4H).

4,4′-Bis(3,4-dicarboxyphenoxy)diphenyl thioether (4). (4) was synthesized according to the literature.[23] Yield: 83%. Mp: 190 °C (DSC peak temperature). FT-IR (KBr, cm^{-1}): 1849, 1767 (C═O), 1284, 1228 (C–O–C). ^{1}H NMR (300 MHz, DMSO-d_6, ppm): 8.108–8.081 (d, J = 8.1 Hz, 2H), 7.588–7.580 (d, J = 2.4 Hz, 2H), 7.553–7.540 (dd, J = 1.2, 3.3, 2H), 7.527–7.498 (d, J = 8.7, 4H), 7.258–7.229 (d, J = 8.7 Hz, 4H).

4,4′-Bis(3,4-dicarboxylphenoxy)diphenyl ether (5). (5) was synthesized according to the literature.[23] Yield: 79%. Mp: 242 °C (DSC peak temperature). FT-IR (KBr, cm^{-1}): 1847, 1777 (C═O), 1270, 1215 (C–O–C). ^{1}H NMR (300 MHz, DMSO-d_6, ppm): 8.101–8.073 (d, J = 8.4 Hz, 2H), 7.563–7.527 (dd, J = 2.4 Hz, 8.4 Hz, 2H), 7.475–7.469 (d, J = 1.8 Hz, 2H), 7.302–7.215 (m, 8H).

2.4. Polyimide synthesis and film preparation

In a 100 mL thoroughly dried three-neck flask, 3 mmol dianhydride was placed in 10 mL of DMAc with mechanical stirring under N_2 atmosphere. After the mixture was completely dissolved, 1 mmol of tetra-amine in 10 mL DMAc was added dropwise through a syringe at 30 °C over 3 h, which was further stirred for 24 h. At the later period of tetra-amine solution addition, the additional DMAc solvent was gradually added into the flask to avoid gel generation and the final solid concentration was controlled at about 5%. Subsequently, 1 g of triethylamine and 3 g of acetic anhydride were added into the polyamic acid solution and maintained at 70 °C for 12 h. The obtained polyimide solution was poured into ethanol to give light yellow precipitate, which was collected by filtration, washed thoroughly with ethanol, and dried under vacuum at 80 °C for 24 h.

The synthesized HBPI powder was dissolved in DMAc at a concentration of 5 wt%. The solution was filtered through G3 sand core funnel device, and poured onto a 10 × 10 cm^2 glass plate, followed by curing at 60 °C for 2 h, 80 °C for 2 h, 100 °C for 1 h, 150 °C for 1 h, 250 °C for 1 h, 300 °C for 1 h. After the temperature gradually cooling to the room temperature, the glass plate was immersing into the water, and the flexible light yellow film was peeled. The HBPI sample for refractive indices measurement was prepared by the solution above mentioned through spin-coating onto silicon wafer at a spin rate of 2000 rpm for 10 s, which was subsequently curing at 80 °C for 10 h.

3. Results and discussion

3.1. Monomer synthesis

The synthesis details of dianhydrides have been described by others, therefore, it was not necessary to repeat again (the corresponding ^{1}H NMR spectra were shown in Fig. S1 to Fig. S5†).

As shown in Scheme 1, the novel tetra-amine monomer was obtained through a four-step synthetic route. First, the nucleophilic substitution reaction of 3,5-dimethoxyphenol and 4,4′-dichlorophenyl sulfone in the presence of potassium carbonate in *N*,*N*-dimethylacetamide (DMAc) gave the intermediate

compound **I**: 4,4′-di(3,5-dimethoxyphenoxy)sulfone. Then the 4,4′-di(3,5-dimethoxyphenoxy)sulfone was performed through the demethylation reaction with borontribromide (BBr_3) in the dichloromethane at low temperature to produce the intermediate compound **II**: 4,4′-di(3,5-dihydroxyphenoxy)sulfone. Subsequently, the intermediate compound **II** was reacted with 2-chloro-5-nitrobenzotrifluoride in the presence of potassium carbonate in *N*,*N*-dimethylacetamide (DMAc) to obtain intermediate compound **III**: 4,4′-di[3,5-di(2-trifluoromethyl-4-nitrophenoxy)phenoxy]sulfone. Finally, the novel tetra-amine monomer was obtained by the reduction of intermediate compound **III** with hydrazine monohydrate and Pd/C in ethanol at boiling temperature.

In ^{1}H NMR spectrum as Fig. 1 shown, the resonation signals of protons in tetra-amine appeared in the region of 5.4–8.0 ppm. As expected, the protons in amino groups resonated at 5.5 ppm. The proton H_1 and H_2 resonance resonated at the farthest downfield region because of the inductive effect of electron-withdrawing sulfonyl group; the H_3 and H_4, *ortho*-oriented to aromatic ether, appeared in the upfield region because of the conjugation effect. Overall, all the protons got their attribution perfectly. In Fig. 2, the amino groups showed a pair of N–H stretching bands at 3469 and 3386 cm^{-1}. The characteristic absorption due to sulfonyl (SO_2) groups at about 1320 and 1160 cm^{-1} are observed. These results clearly confirm that the tetra-amine **IV** prepared herein was consistent with the proposed structure.

3.2. Polymer synthesis

Hyperbranched polyimides were generally prepared from A_2 + B_3 or AB_2 type reactions, while A_2 + B_4 type reaction was rarely studied as a branch point to bring into the hyperbranched polyimide. In this paper, several long-chain synthesized dianhydrides were employed as A_2, while 4,4′-di[3,5-di(2-trifluoromethyl-4-aminophenoxy)phenoxy]sulfone was used as B_4, to synthesize a series of hyperbranched polyimides with anhydride terminals through chemical imidization. The synthesis involved two steps as shown in Scheme 2. The long-chain dianhydride and tetra-amine were condensation

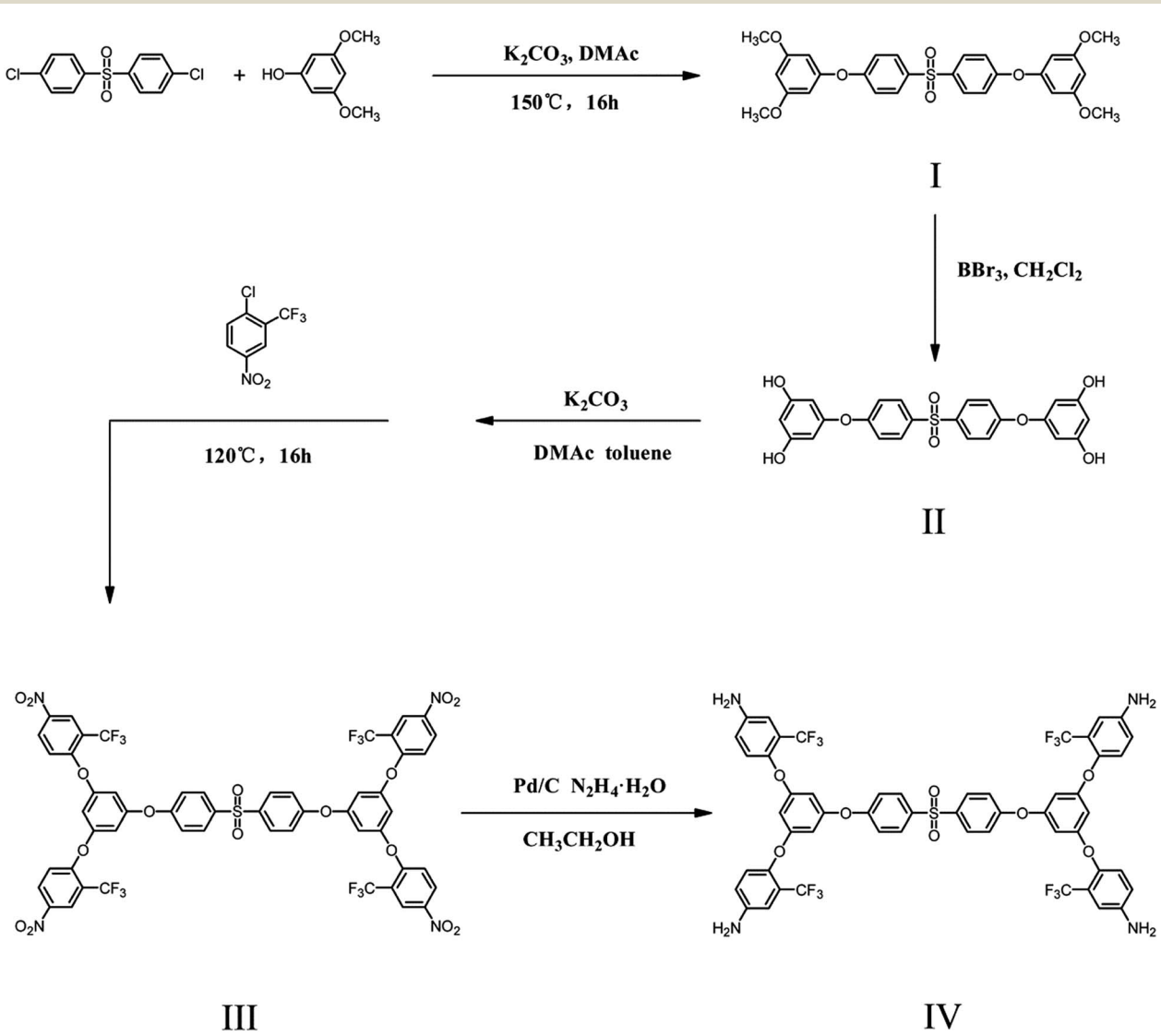

Scheme 1 Synthesis of IV monomer.

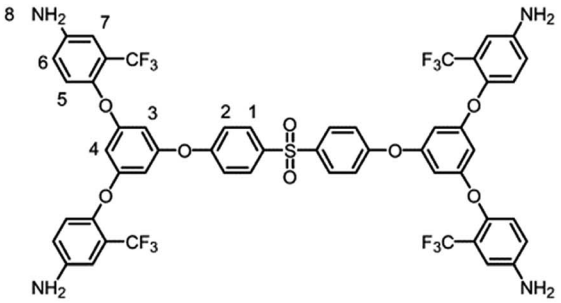

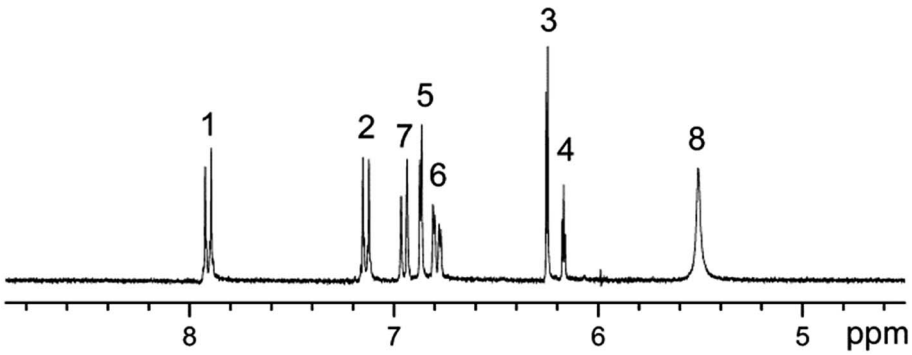

Fig. 1 ^{1}H NMR spectrum of **IV** monomer.

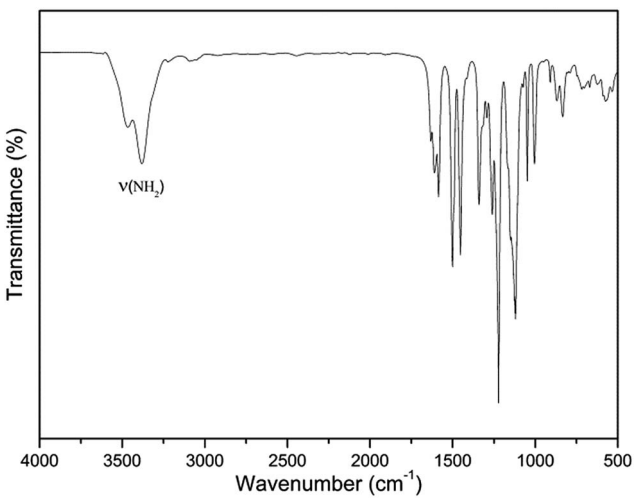

Fig. 2 FT-IR spectrum of **IV** monomer.

polymerized in DMAc to form hyperbranched polyamic acid solution, and subsequently the viscous solution was chemically converted to the final hyperbranched polyimides.

It's known that many factors affect the formation of hyperbranched polyimides, including monomer addition order, monomer molar ratio, concentrations, and reaction temperature.[24] In this study, the HBPIs were synthesized as anhydride terminated to avoid the presence of unstable amino groups, as a result, the tetra-amine should be added into dianhydride solvent. When the monomer **IV** solution was added, the polyamic acid oligomer would form immediately for the high reaction activity of amino and anhydride groups. To avoid the generation of the gel, the tetra-amine should be added slowly enough to ensure its concentration approach zero. It could be deduced that $(2 \times 3^{n-1} - 1)$ number of tetra-amine is required for the condensation reaction with $(2 \times 3^n - 2)$ number of dianhydride molecules, and therefore the appropriate molar ratio between the dianhydride and tetra-amine is 3 : 1 (the molar ratio between anhydride and amine groups in the monomers is 3 : 2).

The structures of HBPIs have been confirmed by FT-IR, as Fig. 3 shown. Absence of the characteristic peaks of polyamic acid around 1660 cm^{-1} and the appearance of the characteristic peaks of the imide ring at 1781 cm^{-1} (C═O asymmetrical stretching), and 1730 cm^{-1} (C═O symmetrical stretching), 1376 cm^{-1} (C–N stretching), 728 cm^{-1} (imide ring deformation) in FTIR spectra suggest a complete conversion of all polyamic acid into the polyimide.[25] In addition, the polyimides did not show any absorption in the range of 3000–3400 cm^{-1}, indicating that the synthesized polyimides were all anhydride-terminated.

The ^{1}H NMR spectrum of PI-2 was shown as an example in Fig. 4. In the ^{1}H NMR spectrum, all the protons resonated in the region of 6.6–8.4 ppm and obtained perfect attributions. The resonance of H_5, H_6 and H_7 shifted to the downfield obviously because of the strong electron-withdrawing effect of carbonyl in the imide ring as a comparison with **IV** monomer. In the range of 4.5–6.0 ppm, the spectrum did not show any proton resonance, indicating that all the polyimide molecules were anhydride-terminated.

3.3. GPC data and intrinsic viscosity

The molecular weights of the HBPIs were obtained through GPC and the results were summarized in Table 1. It is shown that the

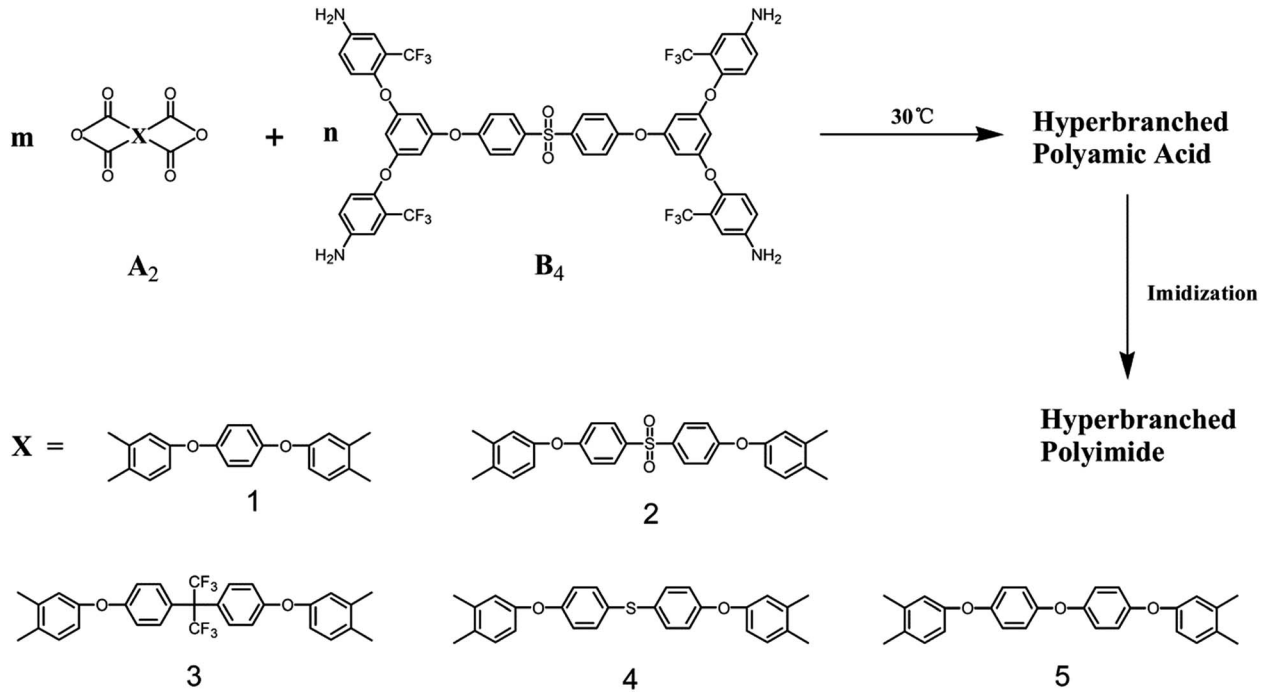

Scheme 2 Polymerization of IV and dianhydride monomers.

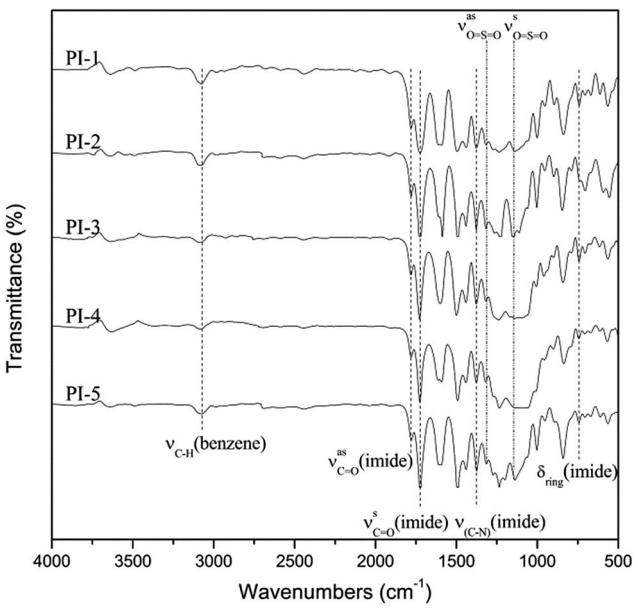

Fig. 3 FT-IR spectra of polyimides.

molecular weights (M_w) of the resulting HBPIs were in the range of 9.17×10^4 to 13.98×10^4 with the M_w/M_n values of 1.73–3.02 and the intrinsic viscosities of the HBPIs were in the range of 1.08–1.17 g dL^{-1}. It is intriguing to observe that the synthesized hyperbranched polyimides showed a relatively high intrinsic viscosity, which gives rise to a little confusion about the common knowledge that the hyperbranched polymers are usually thought to be low in intrinsic viscosity. However, the reason for the phenomenon is unclear yet.[26]

3.4. Solubility

Yin J *et al.* have synthesized several kinds of hyperbranched polyimides derived from 1,3,5-tris(4-aminophnoxy)benzene, while Gao H *et al.* prepared a series of hyperbranched polyimides originated from 1,3,5-tris(2-trifluoromethyl-4-aminophenoxy)benzene.[13,27] The unique difference was the pendent CF_3 group; however, the solubility of the corresponding HBPIs exhibited obvious distinctions. As a result, the CF_3 group affects the solubility of HBPIs significantly.

The solubility properties of synthesized HBPIs which were affected by the chain packing density and intermolecular interaction were tested qualitatively in various organic solvents and the results were collected in Table 2. All the fluorinated polyimides were soluble in aprotic polar solvents at room temperature, such as NMP, DMAc, DMF, and DMSO. Even in less polar solvents, such as THF and pyridine, the polyimides exhibited outstanding solubility. It should be attributed to the presence of the flexible ether structure and the bulky CF_3 substitutes in the tetra-amine, which increased the disorder in the chains and impeded dense chain packing, thus, reducing the intermolecular interactions to enhance the solubility. However, the HBPI films after thermal treatment did not possess favorable solubility. Several anhydride groups at the peripheral of the hyperbranched polyimides tend to decompose at high temperature, and form free radical through pulling off CO and CO_2. The unstable macromolecule free radical would react with adjacent other chain free radical and generate some crosslinking structure.[28]

3.5. Thermal properties

The glass transition temperatures (T_gs) were evaluated by differential scanning calorimetry (DSC) as shown in Fig. 5 and

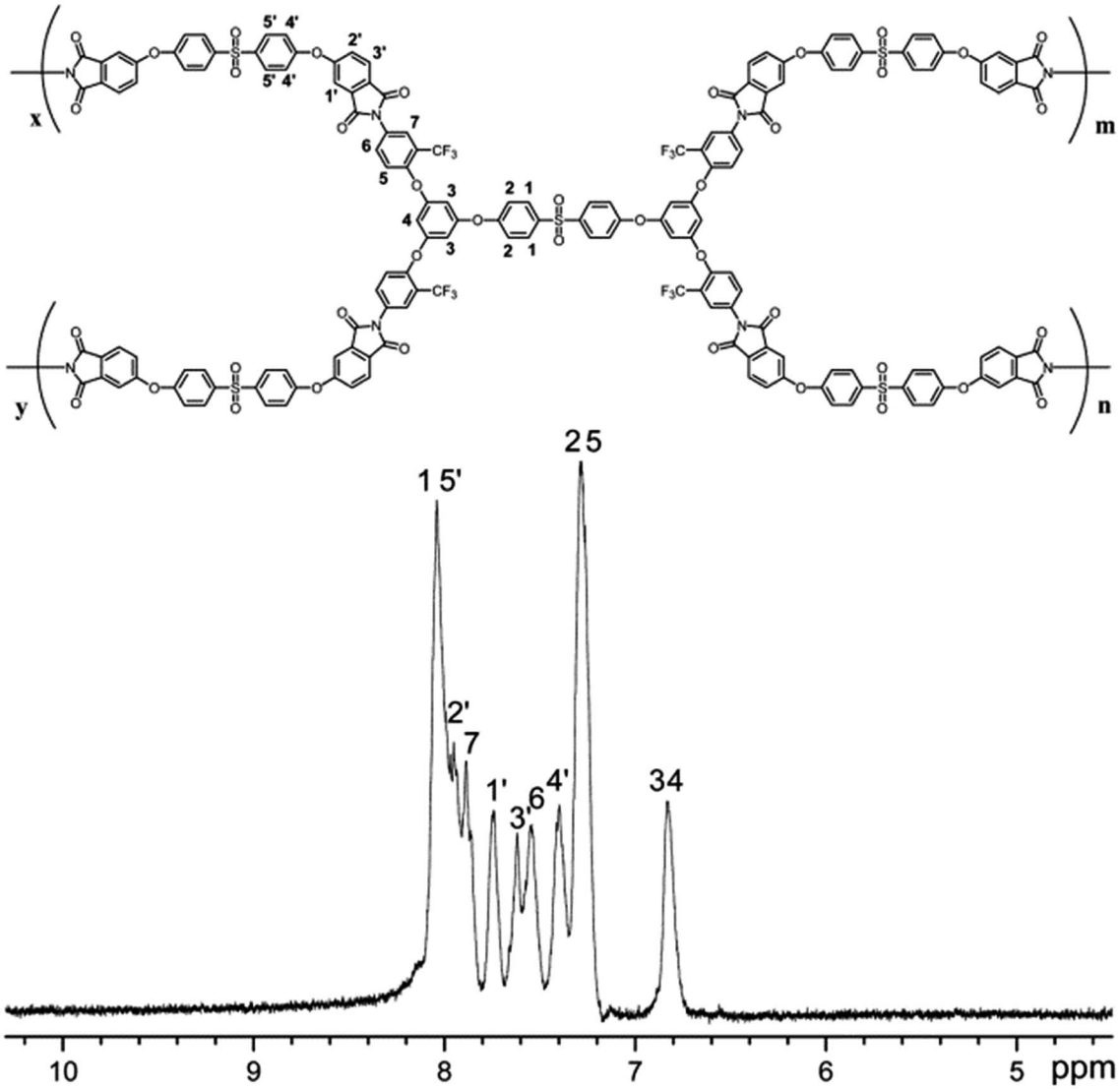

Fig. 4 ^{1}H NMR spectrum of PI-2.

Table 1 GPC data and viscosity

	GPC data			
Polymer	$M_n \times 10^4$	$M_w \times 10^4$	M_w/M_n	$[\eta]_{in}$[a] (g dL^{-1})
PI-1	7.62	13.16	1.73	1.08
PI-2	4.69	10.46	2.23	1.11
PI-3	4.24	10.29	2.43	1.17
PI-4	4.63	13.98	3.02	1.13
PI-5	5.82	9.17	1.58	1.09

[a] $[\eta]_{in}$: Intrinsic viscosity was measured in DMAc at 25 °C.

thermomechanical analysis (TMA), and the results were summarized in Table 3. The T_gs of HBPIs ranged from 230 °C to 242 °C for DSC measurement, and from 232 °C to 263 °C for TMA measurement, indicating that the introduction of pendant trifluoromethyl (CF_3) and ether groups did not decrease T_gs significantly. Moreover, the T_gs from TMA were a little higher than corresponding data from DSC, which could be attributed to the different responding mechanism. The PI-4 and PI-5 showed the lower T_gs than others because of the presence of large amount of flexible thioether or ether linkage in the dianhydride moiety, while the PI-1 exhibited high T_g for the less flexible ether linkage structure compared with others. In addition, PI-2 possessed high T_g for the strong electron-withdrawing sulfonyl groups, which increased the intermolecular interaction. The HBPI films showed coefficient of thermal expansion in the range of 34.4–66.9 ppm K^{-1}. During the curing process, the thioether bonds in PI-4 tend to break and form macromolecule free radicals. The molecular chain would generate more compact structure as the crosslinking which resulted from free radicals. As a result, the PI-4 showed the lowest CTE value (34.4 ppm K^{-1}).[29]

The thermal stabilities of HBPIs were evaluated by TGA under nitrogen as shown in Fig. 6, and the results were

Table 2 Solubility[a] of polyimides

	Solvent[b]								
Polymers	NMP	DMAc	DMF	DMSO	Pyridine	THF	$CHCl_3$	Acetone	Ethanol
PI-1	+	+	+	+	+	+	−	−	−
PI-2	+	+	+	+	+	+	−	−	−
PI-3	+	+	+	+	+	+	+	−	−
PI-4	+	+	+	+	+	+	−	−	−
PI-5	+	+	+	+	+	+	−	−	−

[a] Solubility: the qualitative solubility was test with 10 mg polyimide powder in 1 mL of solvent. (+): soluble at room temperature; (−): insoluble at room temperature. [b] Solvent: NMP, *N*-methyl-2-pyrrolidone; DMAc, *N*,*N*-dimethylacetamide; DMF, *N*,*N*-dimethylformamide; DMSO, dimethyl sulfoxide; THF, tetrahydrofuran.

summarized in Table 3. The decomposition temperatures at 5% weight loss of PIs were recorded in the range of 480–533 °C. All the HBPIs left more than 50% char yields at 800 °C in nitrogen. The TGA results indicated that the synthesized polyimides had fairly high thermal stability. PI-2 showed the worst thermal stability, implying the easy degradation in the heating process for the weak bonding of the C–S bond when the sulfonyl group with strong polarizability appeared. In addition, the PI-4 showed higher char yield obviously compared with others, which should be attributed to the fact that thioether group tends to cause crosslinking in some degree at the atmosphere of stepwise heating.[30,31]

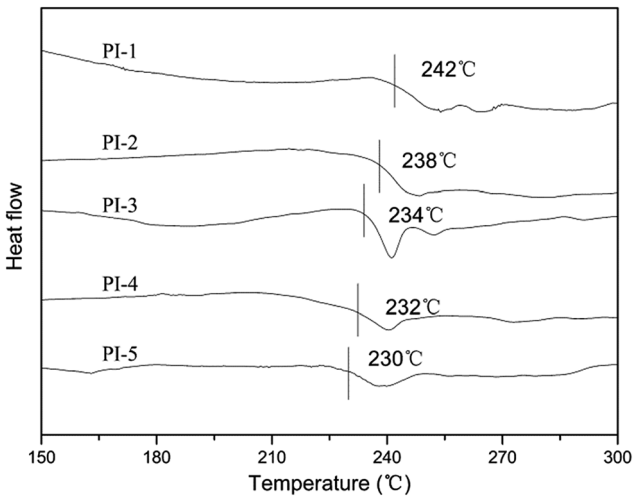

Fig. 5 DSC curves of polyimides.

Table 3 Thermal properties of the polyimides

	T_g[a] (°C)			TGA		
PI	DSC	TMA	CTE[b] (ppm K^{-1})	$T_{5\%}$[c] (°C)	$T_{10\%}$[c] (°C)	R_{w800}[d] (%)
PI-1	242	253	66.9	511	553	51
PI-2	238	263	53.6	480	528	52
PI-3	234	236	48.2	533	553	54
PI-4	232	232	34.4	517	548	71
PI-5	230	236	59.9	510	549	54

[a] T_g: glass transition temperature. [b] CTE: coefficient of thermal expansion. [c] $T_{5\%}$, $T_{10\%}$: temperatures at 5% and 10% weight loss, respectively. [d] R_{w800}: residual weight ratio at 800 °C in nitrogen.

3.6. Mechanical properties

It is known that the hyperbranched polymers do not possess excellent mechanical properties for the lack of intermolecular entanglements. Peter. J *et al.* have demonstrated that the mechanical property of hyperbranched polyimides was affected significantly by the chain physical entanglements, and could be improved through the increase of the linear moiety and the flexibility of relatively rigid branches.[21] Liu *et al.* have discussed the effect of the dianhydride length on the mechanical property of hyperbranched polyimides.[10]

In this article, the synthesized hyperbranched polyimides were intentionally designed to extend molecular length of the dianhydrides to improve the mechanical property. The HBPI films were obtained by casting the DMAc solution of HBPIs onto glass plates followed by thermal curing. As anticipated, the HBPI films exhibited favorable mechanical properties, and the data was listed in Table 4. Overall, the HBPI films showed tensile strength of 91–112 MPa, tensile modulus of 2.14–2.57

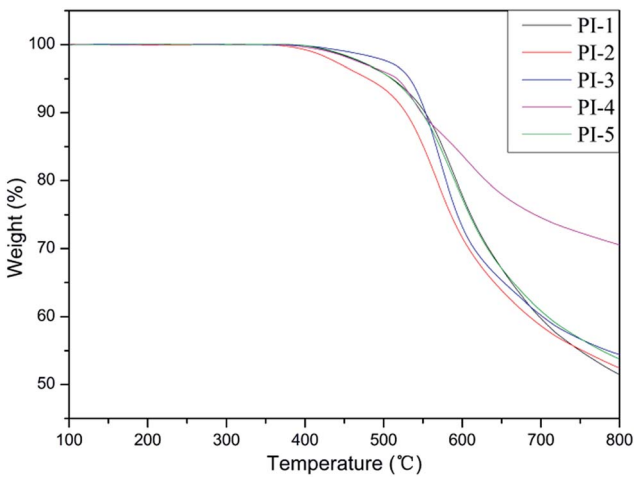

Fig. 6 TGA curves of polyimides.

Table 4 Mechanical properties of polyimides

	Thickness (μm)	Tensile strength (MPa)	Tensile modulus (GPa)	Elongation at break (%)
PI-1	34	91	2.49	6.26
PI-2	39	96	2.14	7.41
PI-3	38	92	2.43	7.99
PI-4	33	94	2.41	7.10
PI-5	45	112	2.57	5.99

GPa, and elongation at break of 5.99–7.99%, indicating that they were strong and tough polymer materials. Note that the HBPIs do not show obvious difference on the mechanical property. This is reasonable for the almost similar monomer molecular length and finally nearly same polymer intrinsic viscosity.

3.7. Optical properties

As a crucial factor for utilization in optical application, the optical transparency of the PI films was characterized by the UV-Vis spectroscopy, and the results were collected in the Table 5, in which the cut-off wavelength (absorption edge, λ_0) values and the percentage transmittance at 800 nm were shown. All the polyimides possessed λ_0 in the range of 353–372 nm, and exhibited high optical transparency of 83–86% at 800 nm. These results are attributable to the reduction of the intermolecular CTC (charge–transfer complex) between alternating electron-donor (tetra-amine) and electron-acceptor dianhydride moieties. The bulky and electron-withdrawing CF_3 groups in the tetra-amine could reduce the CTC formation significantly between polymer chains through steric hindrance and the inductive effect (by decreasing the electron-donating property of the tetra-amine moieties), on the other hand, the ether linkage in the dianhydride would decrease the electron-withdrawing property of the dianhydride.[32,33] In particular, PI-2 and PI-3 exhibited shortest λ_0, which was attributable to the reduction of the intermolecular interactions by the bulky sulfonyl and hexafluoroisopropyl groups in the dianhydride moiety, respectively.

As known, the refractive indices and the birefringence of the polyimides are affected by several factors, including the chain flexibility and linearity, geometry of the repeat units, polarizability and orientation of the bonds in the polymer backbone.[34] As listed in Table 5, the in-plane (n_{TE}) and out-of-plane (n_{TM}) refractive indices of the PI films measured at 632.8 nm range from 1.5802 to 1.6295 and 1.5737 to 1.6223, respectively. The fact that the n_{TE} values of the HBPI films are slightly higher than the n_{TM} ones implies that the chain orientation parallel to the film plane is more dominant than that perpendicular to the plane. The PI-4 exhibited largest n_{av} for the high polarizability of thioether in the dianhydride moiety.[30,31] On the other hand, the PI-3 showed lowest n_{av} for the numerous CF_3, which possess lowest molar refractive index.

The birefringence (Δn) indicated the optical anisotropy of the polymers. As designed, the flexible linkages in the HBPI would result in low molecule chain orientation. Moreover, the configuration of the repeat unit is nonplanar in geometry, which should be attributed to the tetra-amine structure as a branched point. Therefore, the orientation of the chains in the polymer backbone was significantly reduced. The birefringence values ranged from 0.0065 to 0.0079, and all did not show obvious difference for the similar dianhydride moieties.

3.8. Dielectric properties and moisture absorption

The dielectric constants and water absorption of polyimide films were shown in Table 5. The synthesized PIs showed the low dielectric constant at 1 MHz in the range of 2.95–3.31, resulting from the pendant CF_3 groups in the tetra-amine structure, which brought about less efficient chain packing and an increased free volume. In addition, the low polarizability of the C–F bonds also lower the dielectric constant.

Polyimide materials usually exhibit high moisture absorptions for the existence of imide groups, which have a significant influence on the dielectric properties. The trifluoromethyl groups inhibit the absorption of moisture molecules on the surface of the fluorinated polyimides while the bulky volume could decrease the dense packing of the polyimide backbone chains, resulting in the increase of free volume in the polymer that should ensure the polymer to entrap some of the water molecules.[35] These two opposing effects the trifluoromethyl groups offset with each other, to some extent, leading to fluorinated polyimides with lower moisture absorption than the corresponding unfluorinated ones. As expected, the hyperbranched polyimides exhibit low moisture absorptions (0.26–0.57%), which ensures the stable dielectric property of polyimides.

Table 5 Optical properties of the PIs

			Refractive indices and birefringence at 632.8 nm				ε^g	
PI	$\lambda_{cutoff}{}^a$ (nm)	$T_{800}{}^b$ (%)	$n_{TE}{}^c$	$n_{TM}{}^d$	$n_{av}{}^e$	Δn^f	(1 MHz)	w^h (%)
PI-1	364	86	1.6168	1.6101	1.6146	0.0067	3.21	0.34
PI-2	354	84	1.6180	1.6104	1.6155	0.0076	3.24	0.36
PI-3	353	86	1.5802	1.5737	1.5780	0.0065	2.95	0.26
PI-4	372	85	1.6295	1.6223	1.6271	0.0072	3.31	0.57
PI-5	364	83	1.6186	1.6107	1.6160	0.0079	3.15	0.41

[a] λ_{cutoff}: cutoff wavelength. [b] T_{800}: transmittance at 800 nm. [c] n_{TE}: the in-plane refractive index. [d] n_{TM}: the out-of-plane refractive index. [e] n_{av}: average refractive index $[(2n_{TE}{}^2 + n_{TM}{}^2)/3]^{1/2}$. [f] Δn: birefringence $\Delta n = n_{TE} - n_{TM}$. [g] ε: dielectric constant. [h] w: water absorption.

3.9. Polymer condensed structures

The X-ray Diffraction (XRD) was employed to analyze the morphological structure of the HBPIs, as shown in Fig. 7 and Fig. 8. All the HBPIs exhibited amorphous halo for the existence of the featureless lattice in the main chain. This could be ascribed to the fact that the laterally attached CF_3 group in the backbone sterically disrupted the chain packing and inhibited significant chain–chain interactions.[36] On the other hand, the unique globular structure of HBPIs also tends to increase the disorder of chains.

Note that the WAXD patterns of HBPIs showed obvious two dispersion peaks at about 5 and 10°, and the SAXD patterns did not show any peaks. According to the Bragg equation, the high diffraction angle (2θ) means the short distance of molecular chains. In the initial stage of the polymerization, the oligomer would form without defect as dendritic polymers, which might cause large mean intermolecular distance as the meaning of dispersion peak at 5°. As chain growth, several peripheral groups could not polymerize because of the spatial effect, resulting in increased entanglement and decreased interchain distance. Meanwhile, the dispersion at 10° did not show distinct differences with other amorphous PIs, indicating that in the later period of polymerization, the hyperbranched polymers increase the intermolecular entanglement gradually, as linear ones.

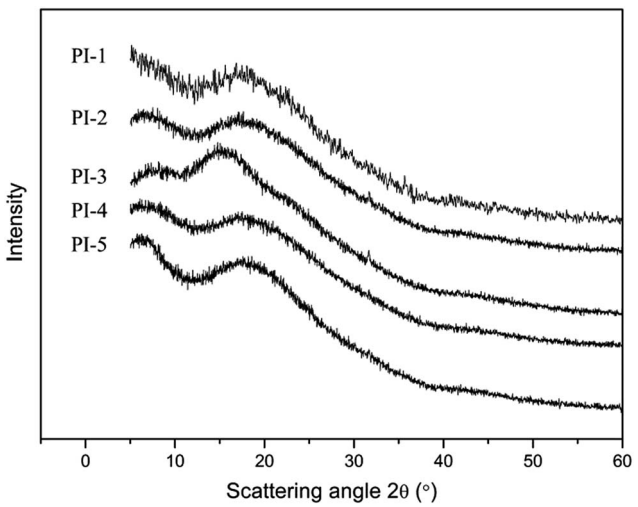

Fig. 7 WAXD patterns of HBPIs.

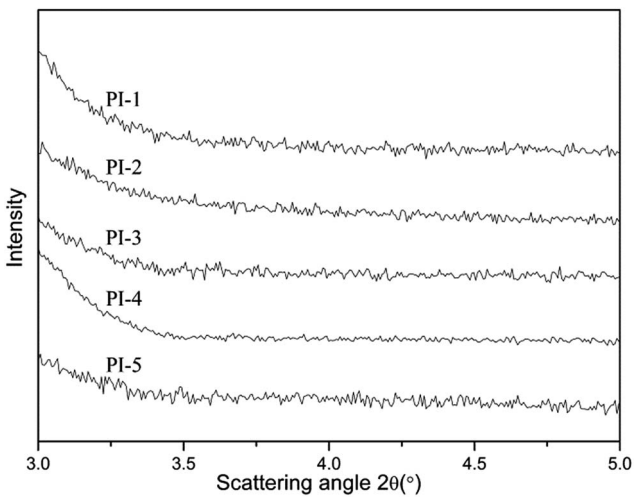

Fig. 8 SAXD patterns of HBPIs.

4. Conclusions

A series of HBPIs were designed and prepared by the polycondensation reaction of the tetra-amine 4,4′-di[3,5-di(2-trifluoromethyl-4-aminophenoxy)phenoxy]sulfone with several aromatic dianhydrides, followed by chemical imidization. The resulted HBPIs exhibit good solubility, excellent thermal stability, low moisture absorption and favorable mechanical properties. As expected, the globular structure endows the HBPIs with low birefringence, while the long-chain dianhydride endows the favorable mechanical property. PI-3 has the lowest n_{av} of 1.5780 for the numerous CF_3 groups, while the PI-4 has the highest n_{av} of 1.6271 for the thioether bonds. All of the properties are desired for advanced optical materials. Thus, the present PIs might find applications as the components for advanced optical device fabrications.

Acknowledgements

The authors are grateful to the National Nature Science Foundation of China (NSFC no. 51573067) for the financial support.

References

1 C. Feger, *Advances in Polyimide: Science and Technology*, CRC Press, 1993.
2 M. Ghosh, *Polyimides: Fundamentals and Applications*, CRC Press, 1996.
3 K. L. Mittal, *Polyimides: Synthesis, Characterization, and Applications*, Springer Science & Business Media, 2013.
4 B. Sillion, R. Mercier and D. Picq, *Synthetic Methods in Step-Growth Polymerisation*, John Wiley & Sons, New York, 2003, p. 265.
5 D. Wilson, H. D. Stenzenberger and P. M. Hergenrother, *Polyimides*, Springer, 1990.
6 S. Ando, T. Matsuura and S. Sasaki, *Polym. J.*, 1997, **29**, 69.
7 M. C. Choi, J. Wakita, C. S. Ha and S. Ando, *Macromolecules*, 2009, **42**, 5112.
8 C. Badarau and Z. Y. Wang, *Macromolecules*, 2004, **37**, 147.
9 A. J. Beuhler, D. A. Wargowski, K. D. Singer and T. Kowalczyk, *IEEE Trans. Compon., Packag., Manuf. Technol., Part B*, 1995, **18**, 232.
10 Y. Liu, Y. Zhang, S. Guan, H. Zhang, X. Yue and Z. Jiang, *J. Polym. Sci., Part A: Polym. Chem.*, 2009, **47**, 6269.
11 K. Han, W. H. Jang and T. H. Rhee, *J. Appl. Polym. Sci.*, 2000, **77**, 2172.
12 S. Ando, *J. Photopolym. Sci. Technol.*, 2004, **17**, 219.
13 H. Gao, C. Yan, S. Guan and Z. Jiang, *Polymer*, 2010, **51**, 694.

14 J. Hao, M. Jikei and M. A. Kakimoto, *Macromol. Symp.*, 2003, **199**, 233.
15 M. Jikei and M. A. Kakimoto, *Prog. Polym. Sci.*, 2001, **26**, 1233.
16 Y. H. Kim, *J. Polym. Sci., Part A: Polym. Chem.*, 1998, **36**, 1685.
17 K. Xu and J. Economy, *Macromolecules*, 2004, **37**, 4146.
18 K. L. Wang, M. Jikei and M. A. Kakimoto, *J. Polym. Sci., Part A: Polym. Chem.*, 2004, **42**, 3200.
19 K. Yamanaka, M. Jikei and M. A. Kakimoto, *Macromolecules*, 2001, **34**, 3910.
20 K. Yamanaka, M. Jikei and M. A. Kakimoto, *Macromolecules*, 2000, **33**, 6937.
21 J. Peter, A. Khalyavina, J. Kříž and M. Bleha, *Eur. Polym. J.*, 2009, **45**, 1716.
22 Y. Zheng, S. Li, Z. Weng and C. Gao, *Chem. Soc. Rev.*, 2015, **44**, 4091.
23 G. Eastmond and J. Paprotny, *Polymer*, 1994, **35**, 5148.
24 J. Fang, H. Kita and K. I. Okamoto, *Macromolecules*, 2000, **33**, 4639.
25 Y. Jin, G. Zeng, D. Zhu, Y. Huang and Z. Su, *Chin. J. Appl. Chem.*, 2011, **28**, 258.
26 J. Hao, M. Jikei and M. A. Kakimoto, *Macromolecules*, 2002, **35**, 5372.
27 H. Chen and J. Yin, *J. Polym. Sci., Part A: Polym. Chem.*, 2002, **40**, 3804.
28 Y. N. Sazanov and L. A. Shibaev, *Thermochim. Acta*, 1976, **15**, 43.
29 Y. Liu, A. Lu and H. Yang, *Polym. Bull.*, 2012, **8**, 74.
30 J. Liu, Y. Nakamura, Y. Shibasaki, S. Ando and M. Ueda, *Macromolecules*, 2007, **40**, 4614.
31 J. Liu, Y. Nakamura, Y. Suzuki, Y. Shibasaki, S. Ando and M. Ueda, *Macromolecules*, 2007, **40**, 7902.
32 C. P. Yang, R. S. Chen and K. H. Chen, *J. Appl. Polym. Sci.*, 2005, **95**, 922.
33 C. P. Yang, S. H. Hsiao and K. H. Chen, *Polymer*, 2002, **43**, 5095.
34 H. Ma, A. K. Y. Jen and L. R. Dalton, *Adv. Mater.*, 2002, **14**, 1339.
35 F. Yang, Y. Li, T. Ma, Q. Bu and S. Zhang, *J. Fluorine Chem.*, 2010, **131**, 767.
36 W. Jang, D. Shin, S. Choi, S. Park and H. Han, *Polymer*, 2007, **48**, 2130.